







Direct powder extrusion (DPE) 3D-printing of mini-tablets for preclinical studies in rodents

Costanza Fratini^{a,1} , Sofia Moroni^{a,1}, Davide De Angelis^b, Mattia Tiboni^a ,
Anna Giulia Balducci^b, Alessandra Rossi^c , Annalisa Aluigi^c, Francesco Amadei^b,
Luca Casettari^{a,*} 

^a University of Urbino Carlo Bo, Department of Biomolecular Sciences, School of Pharmacy, Via Ca le Suore 2, 61029 Urbino (PU), Italy

^b Chiesi Farmaceutici Spa, Preclinical, A&EF Department, Largo Belloli 11/A, 43122 Parma, Italy

^c University of Parma, Department of Food and Drug, Parco Area delle Scienze 27/A, 43124 Parma, Italy

ARTICLE INFO

Keywords:

3D printing
Mini tablets
Small-batch production
Preclinical investigation

ABSTRACT

3D printing (3DP) plays a crucial role in accelerating formulation processes and significantly reduces the time needed to transition from concept to prototype. This technology is particularly valuable as it allows researchers to quickly adjust the structure and composition of dosage forms and efficiently evaluate multiple formulations for safety and efficacy. The following research explores the feasibility of using the direct powder extrusion (DPE) technique to produce 3D-printed mini tablets for eventual *in vivo* preclinical trials in rodents. The DPE method streamlines the manufacturing process into a single step and addresses the limitations commonly associated with Fused Deposition Modeling (FDM). It offers advantages such as customized small-batch production, optimized costs, and minimal waste. This allows pharmaceutical companies to quickly respond to market demands and improve overall product quality through detailed characterization. In this study cellulose-based polymers like Hydroxypropyl Cellulose (HPC-L) and Hydroxypropyl Methylcellulose (HPMC-15LV) were selected as the main matrix excipients, incorporating 10 % w/w of a model drug. The formulations were further optimized to achieve the best flowability and extrudability, as well as the most desirable printing resolution, to produce 3D-printed mini tablets resembling size 9 capsules. Based on the inner diameter of the cannula used for oral administration in rats, tablets measuring $8.6 \times 1.8 \times 1.8$ mm were successfully printed. Thermal analysis (DSC and TGA) and solid-state characterization (FTIR, XRD) were employed to evaluate the physical properties of the powder blends and final 3D-printed products along with the assessment of desirable mechanical features. The successful production of small batches of model 3D-printed mini tablets that are suitable for *in vivo* testing and present comparable release profiles with conventional employed capsules demonstrated the possibility to implement DPE during preclinical development of novel formulations working independently from suppliers.

1. Introduction

3D printing (3DP) is an additive manufacturing technique that has found widespread applications across various fields, including pharmaceuticals, where it has spurred significant research and development in drug delivery (Konta et al., 2017). This innovative approach offers distinct advantages over traditional manufacturing methods by enabling the rapid, accurate, and cost-effective production of complex objects through rapid prototyping (Zema et al., 2017). Moreover, 3DP facilitates the on-demand production of fully customizable dosage forms that vary

in size, shape, release kinetics, and drug loading (Milliken et al., 2024), thereby enhancing their suitability for *in vivo* trials in rodents or eventually other species. In preclinical studies, 3DP may play a pivotal role in accelerating formulation development. It can be employed for quick small-batch production during testing of new drugs, significantly reducing the time from concept to prototype (Tracy et al., 2023). This capability is crucial as it enables researchers to efficiently evaluate multiple formulations for efficacy and safety. Furthermore, the flexibility of the 3DP process empowers researchers to rapidly adjust the composition and structure of dosage forms. This agility facilitates

* Corresponding author.

E-mail address: luca.casettari@uniurb.it (L. Casettari).

¹ Authors equally contributed.

Table 1
Composition of the powder blends containing 10 % w/w caffeine.

Formulation	Matrix Excipient	PEO 100 kDa	Mannitol	PEG 6 kDa
F1	HPC-L	/	/	/
F2		10 %	/	/
F3		/	10 %	/
F4	HPC-SSL	/	/	/
F5		10 %	/	/
F6		/	10 %	/
F7	HPMC HME 15LV	/	/	/
F8		10 %	/	/
F9		/	10 %	/
F9'		/	10 %	5 %
F10		/	/	10 %
F11	HPMC HME 100LV	/	/	/
F12		10 %	/	/
F13		/	10 %	/
F14		/	/	10 %

Table 2
Composition of the powder blends containing 10 % w/w naproxen.

Formulation	Matrix Excipient	PEO 100 kDa	Mannitol	PEG 6 kDa
F15	HPC-L	/	/	/
F16	HPC-SSL	/	/	/
F17	HPMC HME 15LV	/	/	/
F18		10 %	/	/
F19		/	10 %	/
F19'		/	10 %	5 %
F20		/	/	10 %
F21	HPMC HME 100LV	/	/	/
F22		10 %	/	/
F23		/	10 %	/
F24		/	/	10 %

exploration into various release mechanisms and drug combinations, thus optimizing therapeutic outcomes. The small batch production capability of 3DP is a significant advantage in preclinical research. By enabling the cost-effective production of drugs in small quantities, it minimizes waste and reduces costs, particularly beneficial in the early stages of drug development where large quantities are unnecessary (Sánchez-Guirales et al., 2021). This flexibility also allows for the creation of customized doses tailored to specific preclinical study requirements, supporting more precise and targeted research endeavors. Essentially, 3DP through its additive manufacturing approach revolutionizes drug development in pharmaceuticals by enhancing speed, flexibility, and cost-effectiveness. By accelerating formulation development, it supports customization (Pandey, 2020), thereby advancing preclinical studies and paving the way for more efficient clinical trials and eventual commercialization of novel therapies.

Among the various 3DP techniques, direct powder extrusion (DPE) has recently garnered significant interest (Goyanes et al., 2019). DPE streamlines the production process into a single step by allowing the direct feeding and processing of powder or pellet blends into the printer (Fanous et al., 2020; Liu et al., 2019). Specifically, the process involves feeding the material through a hopper, controlled heating, and then extruding the molten material through the nozzle. Currently, when testing *in vivo* oral dosage forms, small empty capsules are purchased from suppliers and manually filled with the selected formulation and administered to rats via a dosing cannula or syringe. The application of DPE to develop mini tablets for oral administration in rodents *in vivo* studies offers pharmaceutical companies several advantages: i) customized production in small batches, ii) optimized costs, iii) minimized waste (Pistone, 2023; Pistone, 2022) iv) independent work from suppliers. Flexibility in customizing tablets in terms of size, shape, and release characteristics enhances the accuracy of *in vivo* trials reaching ethical requirements. Moreover, the rapid prototyping enabled by DPE speeds up the manufacturing of pharmaceutical formulations (Boniatto,

2021), enabling companies to promptly respond to market needs and improve overall product quality through detailed characterization.

The aim of this project is to investigate the potential application of DPE technique to develop small batches of mini tablets that could be administered orally to rats for *in vivo* studies during the development of new drugs. For this reason, 10 % of a model drug (e.g., caffeine or naproxen) was incorporated. Having different melting temperatures, caffeine and naproxen were chosen as models, thus an evaluation of the different thermal behaviours in the molten polymer matrices was possible. A variety of cellulose-based excipient matrices were screened to identify the most suitable for the DPE 3DP process in terms of extrudability and printability. Additionally, the formulation and printing parameters (e.g. addition of plasticizing agents, printing temperatures, nozzle diameter) were adjusted and optimized to provide a model platform that can be easily employed according to the needs to produce 3D-printed mini dosage forms and loaded with drugs that must be tested *in vivo*. Furthermore, the most suitable formulations were thoroughly characterized. Thermal gravimetric analysis (TGA) and differential scanning calorimetry (DSC) were conducted to assess the thermal stability and suitability of the 3DP process towards both the raw materials and the final products. Crystallinity of the system evaluated through Powder X-Ray Diffraction (XRPD) and scanning electron microscopy (SEM) was employed to observe the morphology of the 3D-printed products. Additional characterization included Fourier-transform infrared spectroscopy (FTIR), mass uniformity, drug loading, and dissolution studies. The mechanical properties of the mini tablets were also investigated.

2. Materials and methods

2.1. 2.1. Materials

Hydroxypropyl celluloses (HPC-L MW 140 kDa, and HPC-SSL MW 40 kDa) were obtained from Nippon Soda (Japan), while hydroxypropyl methylcellulose (AFFINISOL™, HPMC HME 15LV and AFFINISOL™, HPMC HME 100LV) from DuPont (USA). Caffeine from Carlo Erba (Italy) and naproxen from BLD Pharm (Germany) were selected as model drugs. Polyox WSR N10 (PEO, MW 100 kDa) was purchased from Colorcon (UK); while mannitol from Farmalabor (Italy) and PEG 6 kDa from Merck (Germany). The salts (NaCl, KCl, Na₂HPO₄·2H₂O, KH₂PO₄) employed for preparing PBS, methanol and formic acid were purchased from Merck (Italy). All solvents used were analytical grade.

2.2. Selection of printable cellulose-based polymeric excipients

Prior printing, each batch (5 g) was prepared by weighing the components, drying overnight at 40 °C, and finally the blend was homogeneously shaker mixed for 15 min at 100 rpm (Galena Top powder mixer, Ataena, Italy). The prepared blend was directly fed into the printing unit (Tumaker NX Pro, Spain) prior preheating the equipment approximately for 15 min. After each trial, the printhead was disassembled and cleaned preventing cross-mixing between the formulations.

Firstly, the extrudability was evaluated, considering formulations “extrudable” when a good flowability and a uniformity of filaments coming out from the nozzle were observed. Subsequently, the extrudable formulations were considered “printable” when the layer-by-layer deposition of the molten material led to the production of the desired design.

The matrix excipient was first blended with 10 % w/w of the selected model drug corresponding to administrable rodent dose of 1.5 mg/unit during preclinical studies. If the formulation was not extrudable or the printability was not adequate, different percentages of additional excipients were considered according to the necessities. Mannitol, PEO 100 kDa or PEG 6 kDa were added as plasticizer to control the flowability of the material and/or as binders to enhance the layer-layer

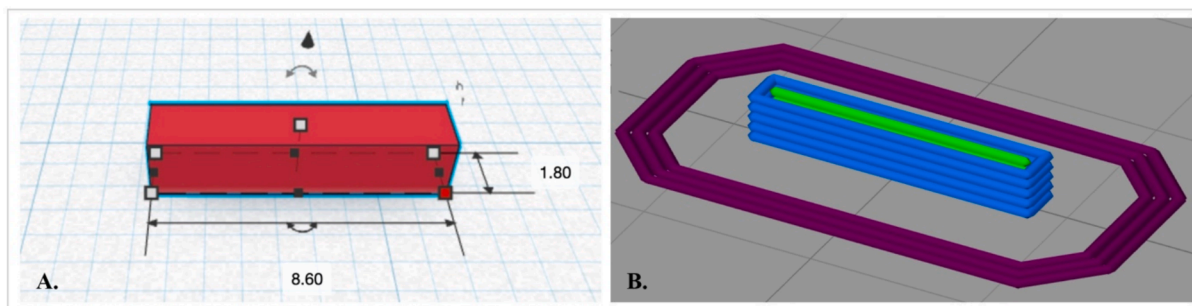


Fig. 1. A) CAD design of the mini tablets; B) printing preview of the CAD design after slicing.

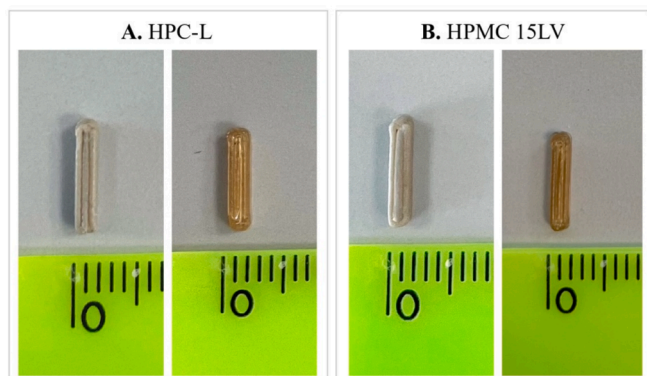


Fig. 2. Top view of the printed mini tablets: A) HPC-L-based formulations loaded with caffeine (F3, left) and naproxen (F15, right); B) HPMC 15LV-based formulations loaded with caffeine (F9, left) and naproxen (F19, right). Scale is expressed in cm.

adhesion. Table 1 and Table 2 report the composition of each formulation tested with 10 % w/w of caffeine or naproxen, respectively.

2.3. Optimization of the printing process parameters

Since the mini tablets are intended for eventual *in vivo* studies in rats, it is necessary to choose the appropriate size and shape. Thus, based on the cannula's inner dimension that is employed for the administration of a size 9 capsule by gavage, a rectangular shape (8.6 mm length x 1.8 mm height x 1.8 mm width), was designed using a freeware CAD tool. The .stl file was converted to G-code using Simplify3D software (Fig. 1). The optimization of the printing parameters was performed using a nozzle of 0.2 mm diameter, to achieve a better resolution of the printed form. The printing temperature was set at 170/180 °C and to improve the adhesion, the bed was heated at 80 °C. When the adhesion of the material to the printing bed was still poor, a polypropylene (PP) adhesion sheet was added. The infill density was kept at 100 % and different infill patterns were investigated (e.g., rectilinear, aligned, grid). The aligned was considered the most suitable, providing a good structural accuracy in terms of final outcome of the mini tablet. The default speed was set at 5 mm/s, while the travel speed was 50 mm/s. Three layers of skirt were added to provide continuity to the material's flow.

2.4. Powder blend uniformity

To confirm the homogeneity of the formulation, random samples were collected after mechanical mixing and analyzed using UV-Vis spectrometry (UV-1900 i, Shimadzu, Tokyo, Japan). Specifically, the powder blends were dissolved in PBS (1 mg/mL) and stirred until complete dissolution. The spectrum mode, in the range 200–400 nm was applied for the analysis. The intensity of the resulting absorbance was

visually compared among three replicates from the same formulation.

2.5. Differential scanning calorimetry (DSC) and Thermogravimetric analysis (TGA)

The thermal behaviour of the pure model drugs, excipients, the physical blends and the final 3D printed mini tablets was investigated through DSC (DSC 6000, Perkin Elmer, USA), and TGA (TGA 4000, Perkin Elmer, USA) analyses. Specifically, for the DSC measurements, approximately an average mass of 5–10 mg of sample was placed in an aluminium pan and heated up from 25 °C to 275 °C at 10 °C/min. Nitrogen flow rate was kept at 30 mL/min. While for TGA analysis, scans were run from 25 °C to 550 °C, at a speed rate of 10 °C/min, using nitrogen as purge gas. Data collection and analyses were performed using Pyris Manager software (Perkin Elmer, USA).

2.6. Fourier-Transform infrared spectroscopy (FTIR)

FTIR (Spectrum Two, Perkin Elmer, MA, USA) was employed to investigate the chemical composition of the physical blends and the pointlets; and compare it with the raw materials. Measurements were carried out at 400–4000 cm^{-1} with a resolution of 4 cm^{-1} and a total of 64 scans.

2.7. X-ray diffraction (XRD)

The solid state of 3D printed forms was investigated by X-ray powder diffraction with Empyrean V2.0 (Malvern Panalytical, Netherlands) equipped with Cu radiation source (Cu K α 1.5406 Å), generator voltage set to 40 kV and the current to 40 mA. Samples were acquired under transmission mode spinning with revolution time 0.5 s. The measurements were scanned over 2Theta range from 2° to 45°, step size 0.02°, soller slit 0.02 rad, divergence slit 1/2°, antiscatter slit 1/2°.

2.8. Morphological characterization by scanning electron microscopy (SEM)

The morphology of the 3DP mini tablets was observed with a SEM microscope (FEI, Hillsboro, OR USA). The instrument was employed in low-vacuum mode, applying a specimen pressure chamber of 0.8 mbar and an acceleration magnitude of 25.0 kV. The magnitude ranged between 100 and 255 \times , while the working distance ranged between 8.7–9.6 mm. The images were performed using the large field detector (LFD).

2.9. Uniformity of dosage units

Mass uniformity was assessed according to the method described in the European Pharmacopoeia (Eur. Ph. XI Ed.) for uncoated tablets of mass <80 mg, the deviation is set at ± 10 % from the average. A total of 20 dosage units, taken randomly, were analyzed.

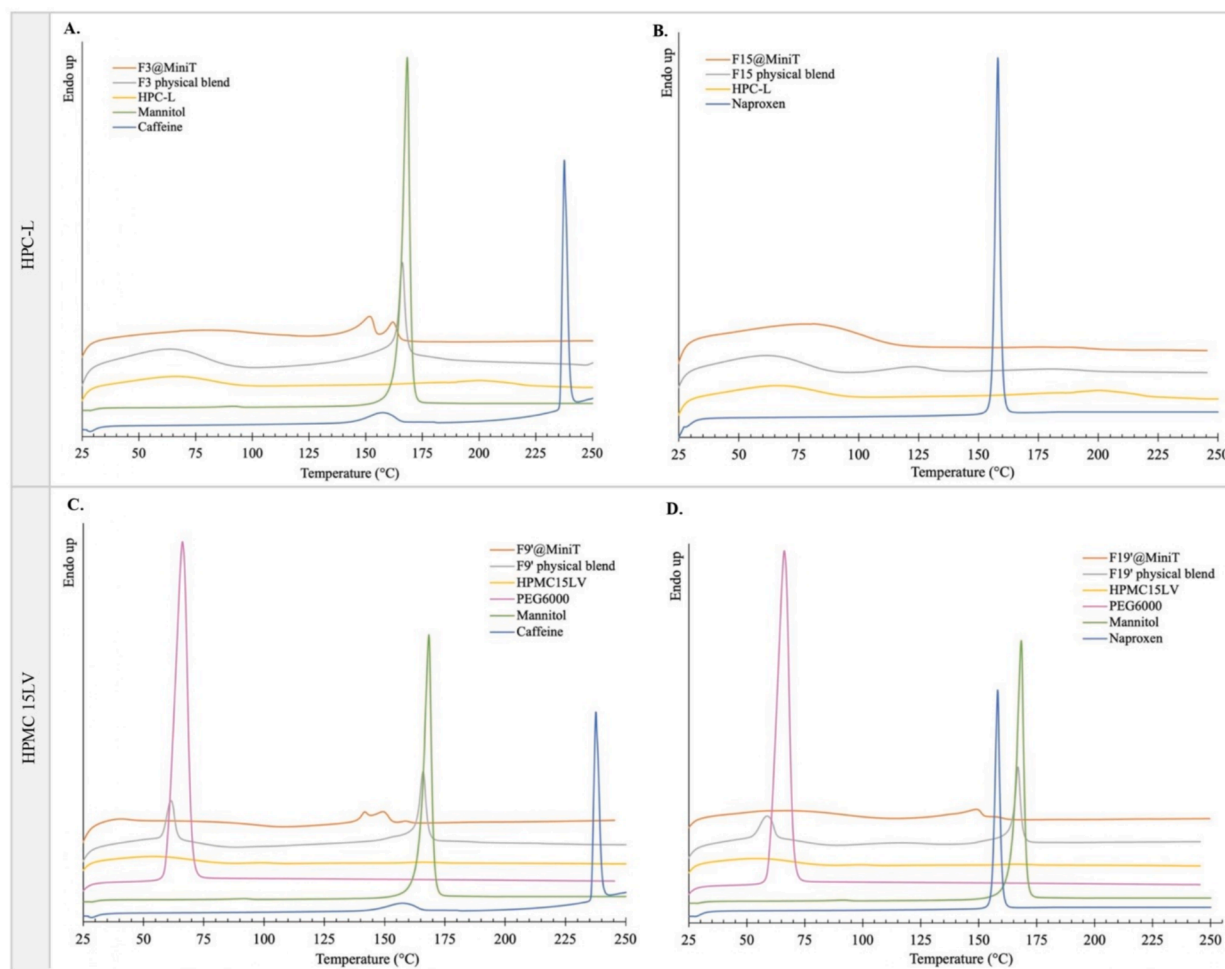


Fig. 3. DSC thermograms of caffeine (A and C) and naproxen (B and D) loaded formulations in the two different polymer matrices.

2.10. Drug content

For naproxen-loaded mini tablets, the effective drug loading was quantified using UV–Vis (Shimadzu UV-1900i, Shimadzu, Tokyo, Japan) dissolving the mini tablets in PBS. The analysis was conducted in spectrum mode, and the peak absorbance was evaluated at 230 nm. HPLC (Agilent 1260 Infinity II, Agilent, USA) was employed for quantitative detection of caffeine. The analysis was conducted using an Agilent Zorbax Eclipse Plus C18, 150 × 4.6 mm, 5 μm column (Agilent, USA), at room temperature. 0.5 % formic acid (FA) in water and methanol (60:40) were selected as mobile phases, setting the flow rate at 1 mL/min and the injection volume at 20 μL. The detection signal was recorded at 274 nm. Calibration curves were also performed, and linearity was guaranteed in the interval of 1–40 μg/ml and 0.5–10 μg/ml in case of caffeine and naproxen, respectively, with the R^2 values equal to 0.9999 in both cases.

2.11. In vitro drug release

The cumulative drug release profile of the drug from the 3DP mini tablets was evaluated adapting the method described in the European Pharmacopoeia (Dissolution Test, Eur. Ph. XI Ed.). The analysis was carried out using a PTWS 120D Dissolution apparatus (Pharma Test, Germany) equipped with a basket stirring tool. Stirring was fixed at 60 rpm and the temperature kept at 37 °C. To mimic the physiological condition, different pH media were used. Specifically, the mini tablets were immersed in 75 mL of HCl 0.1 N pH 1.2 for the first 2 h, mimicking the stomach acidity, then 25 mL of Na₂HPO₄ 0.2 M were added and pH

adjusted to 6.8 with minimum amount of NaOH 2 M simulating the transit to the intestine until complete dissolution of the mini tablet. Time points were recorded each 15 min for the first hour and then each 30 min. Samples of 1 mL were withdrawn at each time point and then replaced with fresh medium. Quantification studies were carried out using UV–vis for naproxen and UV-HPLC for caffeine. Analytical methods are described in section 2.10. The analysis was carried out in triplicate. Also, for each formulation, size 9 capsules were manually filled with the powder blends and the drug release profile was assessed at the same conditions described above.

2.12. Mechanical properties

A compression test was performed to assess the mechanical properties of the 3D printed mini tablets with a TA.XTplus Texture Analyzer, (Stable Micro Systems, Surrey, UK) equipped with a 50 Kg load cell. Tests were conducted using a compression probe of 2 mm diameter, a constant compression speed of 0.03 mm/sec, and a trigger force of 100 g, to achieve a strain of 100 %. The analysis was carried out at room temperature and for a total of five samples for each formulation. Data was collected as stress vs strain. The peak force (N) registered at 100 % strain and the Unconfined Compressive Strength (UCS, MPa) were defined, while the Young's Modulus (YM, MPa) and the Yield Point (YP, MPa) were determined from engineering the stress/strain curves.

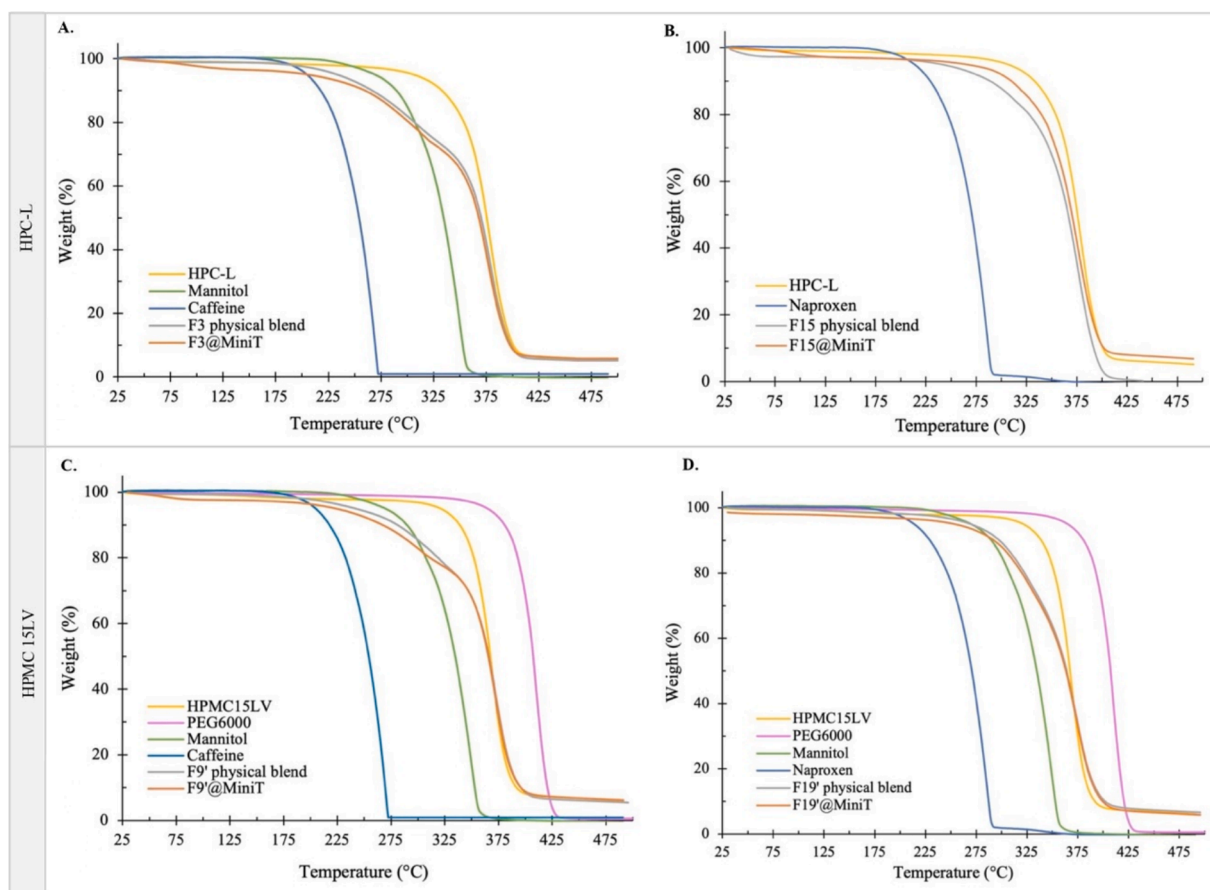


Fig. 4. TGA thermograms of caffeine (A and C) and naproxen (B and D) loaded formulations in the two different polymer matrices.

3. Results and discussion

3.1. Selection of printable cellulose-based polymeric excipients

In the identification of the optimal formulation, appreciable flowability is a fundamental prerequisite for a good resolution of the printing performance. Hence, the extrudability and printability were evaluated for each blend.

During extrudability tests, for HPC-based formulations (HPC-L and SSL) loaded with caffeine, F1 and F4, extrusion was difficult and not constant, being characterized by under-extrusion followed by over-extrusion, suggesting the need for an additional excipient to facilitate and control the flow. However, PEO 100 kDa (F2 and F5), was not appropriate, providing a plasticizing effect without controlling the amount of extruded material. Surprisingly, the addition of mannitol (F3 and F6) showed promising results. On the contrary, when incorporating naproxen to HPC-L (F15 and F16), no additional excipients were needed suggesting that the drug provided itself a plasticizing effect to the blend.

Two different grades of HPMC at lower and higher molecular weight (15LV and 100LV, respectively) were tested. Formulations containing 10 % w/w of the drug, caffeine or naproxen, (F7, F11, F17, F21) had a good extrudability at the selected temperatures but the filament resulted to be very stiff. The addition of 10 % mannitol (F9, F13, F19, F23) resulted in a good flow of the material through the nozzle along with a nice filament consistency. Conversely, when PEO 100 kDa was added to the blend, a loss of the control over the flow rate, that turned out to be too slow, occurred; thus, formulations F8, F12, F18, F23 were discarded. PEG 6 kDa was also investigated as a plasticizing agent (Alhijaj et al., 2016) for the HPMC-based formulations (F10, F14, F20, F24) but it led to a very sticky blend that clogged the nozzle during the extrusion. Overall, the formulations containing HPMC at lower molecular weight

(15LV) resulted in a more controlled and smooth extrusion through the nozzle. Thus, it was selected as the best main matrix excipient over HPMC at higher molecular weight.

Taking into consideration the extrudability test, a preliminary printing trial was performed with the selected formulations. HPC-L based compositions (F3 and F15) provided a superior accuracy of the design over HPC-SSL (F6 and F16), while for HPMC-based formulations, the good extrudability did not lead to a good outcome of the printing process. This was due to a quick cooling of the filament and complete lack of adhesion to the printing bed and layer-to-layer. Hence, the addition of 5 % w/w of PEG 6 kDa to formulations F9, and F19 was selected to enhance the “stickiness” of the blends resulting in a good layer adhesion and printing accuracy. Thus, formulations F3, F9', F15 and F19' were selected as the most suitable candidates for the manufacturing of the mini tablets loaded with the respective model drug. The printed products are represented in Fig. 2. After printing, the devices were measured using a digital calliper (Mitutoyo, Japan) and a good accuracy to the selected CAD dimension was observed.

3.2. Powder blend uniformity

To evaluate the homogeneity of the powder blends, random samples (triplicate) of the same formulation were collected after mechanical mixing. For all the formulations, HPC-L and HPMC 15LV-based, the resulting intensity of the UV bands overlapped, confirming the homogeneity of the mixtures (data not shown).

3.3. Differential scanning calorimetry (DSC) and Thermogravimetric analysis (TGA)

DSC analysis was carried out to assess the thermal stability of the

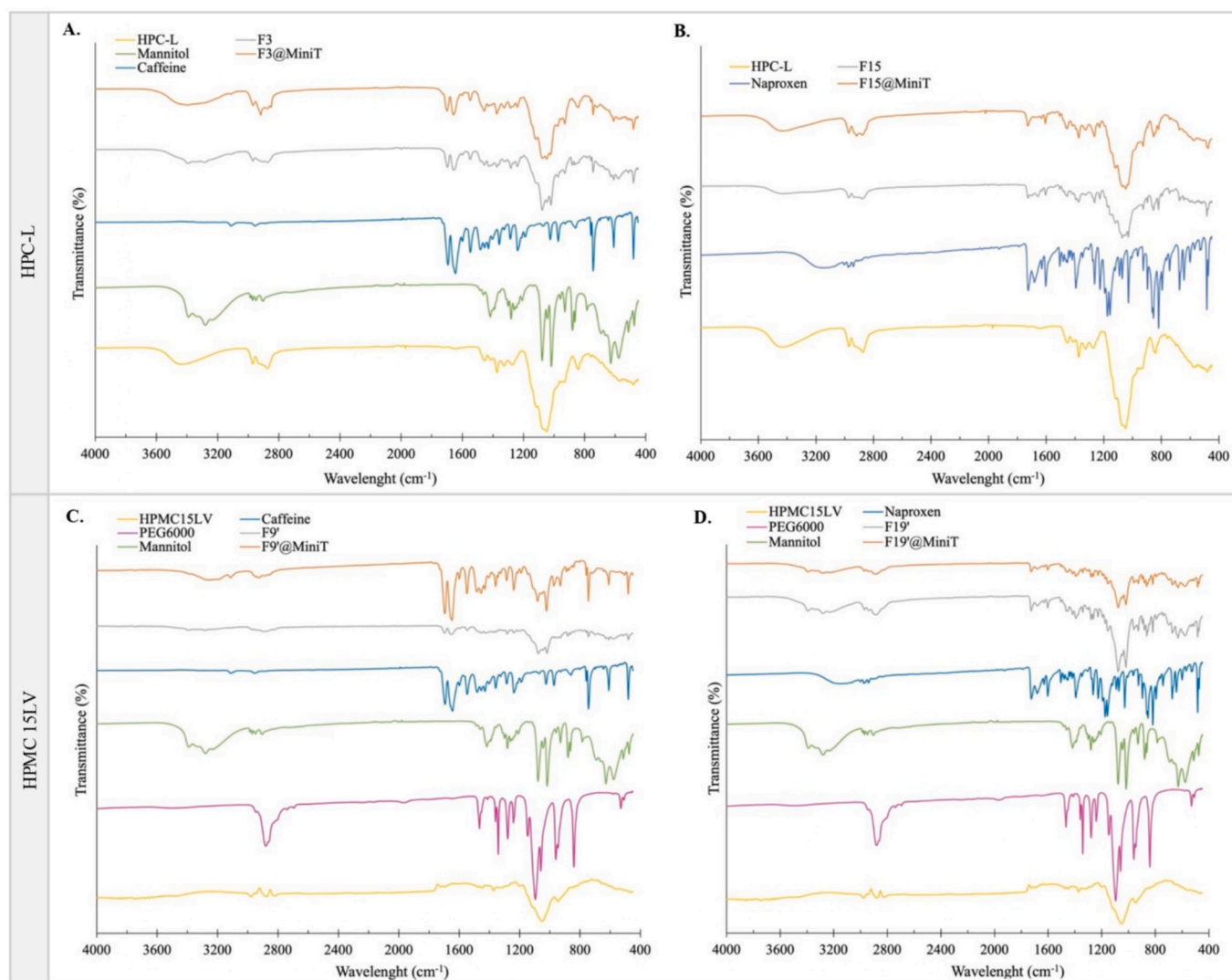


Fig. 5. FTIR spectra of the raw materials, physical blends and 3DP mini tablets. Caffeine-loaded formulations F3 and F9' (A and C), naproxen-loaded formulations F15 and F19' (B and D) in the two different polymer matrices.

excipients and APIs in the most promising formulations at the operating temperatures and after printing. Thermograms are reported in Fig. 3. Naproxen shows its endothermic peak, related to the melting at $T_p = 158.14$ °C while anhydrous caffeine is known to exist in two polymorphic forms, form I, $T_p = 237.73$ °C and form II, $T_p = 158.88$ °C (Mazel et al., 2011; Dichi et al., 2014), explaining the presence of the two endothermic peaks in the thermograms. Mannitol and PEG 6 kDa show their melting peaks at $T_p = 168.16$ °C and $T_p = 66.57$ °C, respectively. Cellulose-based polymers are instead amorphous and glass transition temperatures are hardly detectable as previously reported (Luebbert et al., 2021; Pöstges et al., 2023; Larsen et al., 2024). Thermograms display a broad endothermic event at low temperatures $T < 100$ °C which can be attributed to the evaporation of the moisture absorbed (Patel and Serajuddin, 2022). The peak is anyway weak as the amount of water incorporated is very low due to the overnight drying of the physical blends.

When considering the physical mixtures and 3DP mini-tablets, significant changes in the thermal behaviour are detectable. The naproxen-based formulations (Fig. 3, B and D) show a depression, in terms of temperature and intensity, of the peaks relative to the drug and excipients. This phenomenon is well explained in the literature and it's a symptom of a strong physical interaction between the polymer matrices and the drug, suggesting a good miscibility, where the polymer acts as

the "solvent" and the drug as the "solute" of the mixture (Kissi et al., 2021). Indeed, the resulting 3DP tablets show a complete amorphous state (HPMC 15LV-based tablets present a small endothermic peak probably due to the presence of a low amount of mannitol still in the crystalline form). This is also because the printing temperatures selected are higher than the melting temperature of the drug. DSC thermograms were also confirmed through the XRD analysis and SEM imaging (sections 3.5 and 3.6).

Caffeine-based formulations (Fig. 3, A and C) also display a reduction, in terms of temperature and intensity of the peaks, suggesting a good miscibility of the drug and excipients. Moreover, although caffeine melts at higher temperatures than the printing conditions, the "molten environment" allows the API to easily dissolve. Still, after cooling to room temperature, caffeine recrystallizes quickly (Fanous et al., 2020), also explaining the lack of total amorphization of the drug. Specifically, in formulation F3, caffeine recrystallizes in form I, while in F9' it is present in form II, as assessed through the XRD analysis (section 3.5).

Since the materials are exposed to high temperatures during the 3DP manufacturing process, it is essential that all formulations are processed at conditions that are clearly below the decomposition critical points; ideally, at the lowest feasible processing temperatures (Pflieger et al., 2024). The primary benefit of DPE over FDM 3DP is that the powder blends only need to go through the hot stage once because creating the

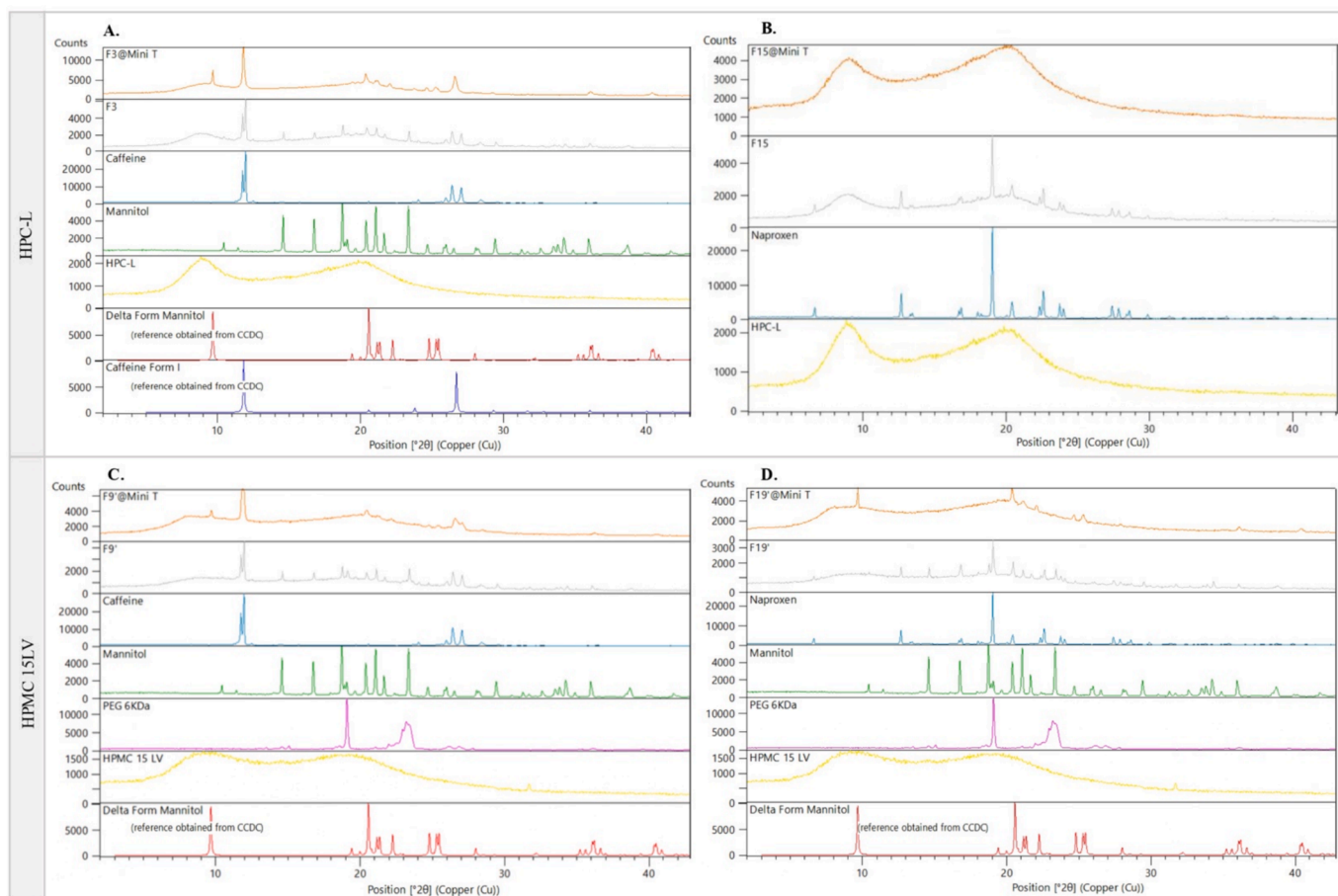


Fig. 6. XRPD diffractograms of the raw materials, physical blends and 3DP mini tablets. Caffeine-loaded formulations F3 and F9' (A and C), naproxen-loaded formulations F15 and F19' (B and D) in the two different polymer matrices.

filament is not a required step.

Based on the weight variations, the TGA thermograms of the active ingredients, excipients, physical mixtures and 3DP mini tablets were examined (Fig. 4). It is evident that the printing temperatures, which range between 170 °C and 180 °C, are far below these critical points. Until 200 °C, indeed, a negligible weight loss was observed for all samples (1.2–2.3 %, due to the release of the moisture absorbed), demonstrating the chemical stability of the materials during the printing process.

3.4. Fourier-transform infrared spectroscopy (FTIR)

FTIR spectra were collected from analyzing the raw materials (excipients and APIs), the powder blends and final 3D printed tablets, as shown in Fig. 5. All the significant peaks observable in the spectra are confirmed with the ones found in literature. HPC-L and HPMC 15LV show their significant peaks around 3200–3400 cm^{-1} , broadband, due to the O–H stretching vibrations in the pyranose ring of the sugar, at 2926 and 2856 cm^{-1} attributed to the C–H asymmetric and symmetric vibrations, and a broad band at 1050 cm^{-1} due to the C–O–C asymmetric stretches (Zaltariov et al., 2020). In the PEG 6 kDa spectrum, the peak at 1100 cm^{-1} is due to the stretching vibration of C–O–C bonds, while the strong peaks around 2800–2900 cm^{-1} to the stretching vibrations of C–H and OH functional groups, respectively (Zahir, 2021; Shao, 2020). Mannitol spectrum displays the main peaks at 3310 cm^{-1} (broadband, O–H stretching vibrations), at 1348 cm^{-1} and 1080 cm^{-1} (C–H and C–O stretching vibration respectively) (Burger et al., 2000). Caffeine has its characteristic peaks at 1670 cm^{-1} (C=O stretching), and at 1638 cm^{-1} (C=N stretching) of the xanthine ring while naproxen spectrum shows a

broad band around 3300–3200 cm^{-1} due to the O–H stretching vibrations and a significant peak at 1555 cm^{-1} characteristic of the stretching vibration of the COOH functional group (Li et al., 2013). Both the spectra of the powder blends and the final 3D printed tablets feature the main peaks of the raw materials (excipients and API), and no unknown peaks appear, nor significant ones disappear, suggesting a good compatibility among the excipients and APIs but also within the manufacturing method.

3.5. X-ray diffraction (XRD)

X-Ray diffraction spectra were acquired on the final 3D printed forms, under transmission mode. Looking at Fig. 6-A, in formulation F3, it is clear the presence of both caffeine recrystallized in form I and Delta form of mannitol. This is mainly caused by the temperatures reached by the printing process (170–180 °C) which are higher than the melting temperatures of caffeine form II (present in the physical powder blends) and Alpha form of mannitol, leaving only the two polymorphs described above as present in the final 3D printed form. This behaviour gives us also the indication that molten HPC-L has a “solvent effect” on caffeine. Fig. 6-C still shows in F9' the presence of recrystallized Delta form of mannitol, but less intense than in F3, and form II of caffeine instead of form I, suggesting that the presence of PEG 6 kDa and HPMC 15LV lower the “solvent effect” of the polymer matrix on caffeine.

On the other hand, the analysis of F15 shows a completely amorphous diffraction pattern (Fig. 6-B) while in F19' is still present some crystallinity related to recrystallized Delta form of mannitol (Fig. 6-D), as previously noticed during the thermal analysis.

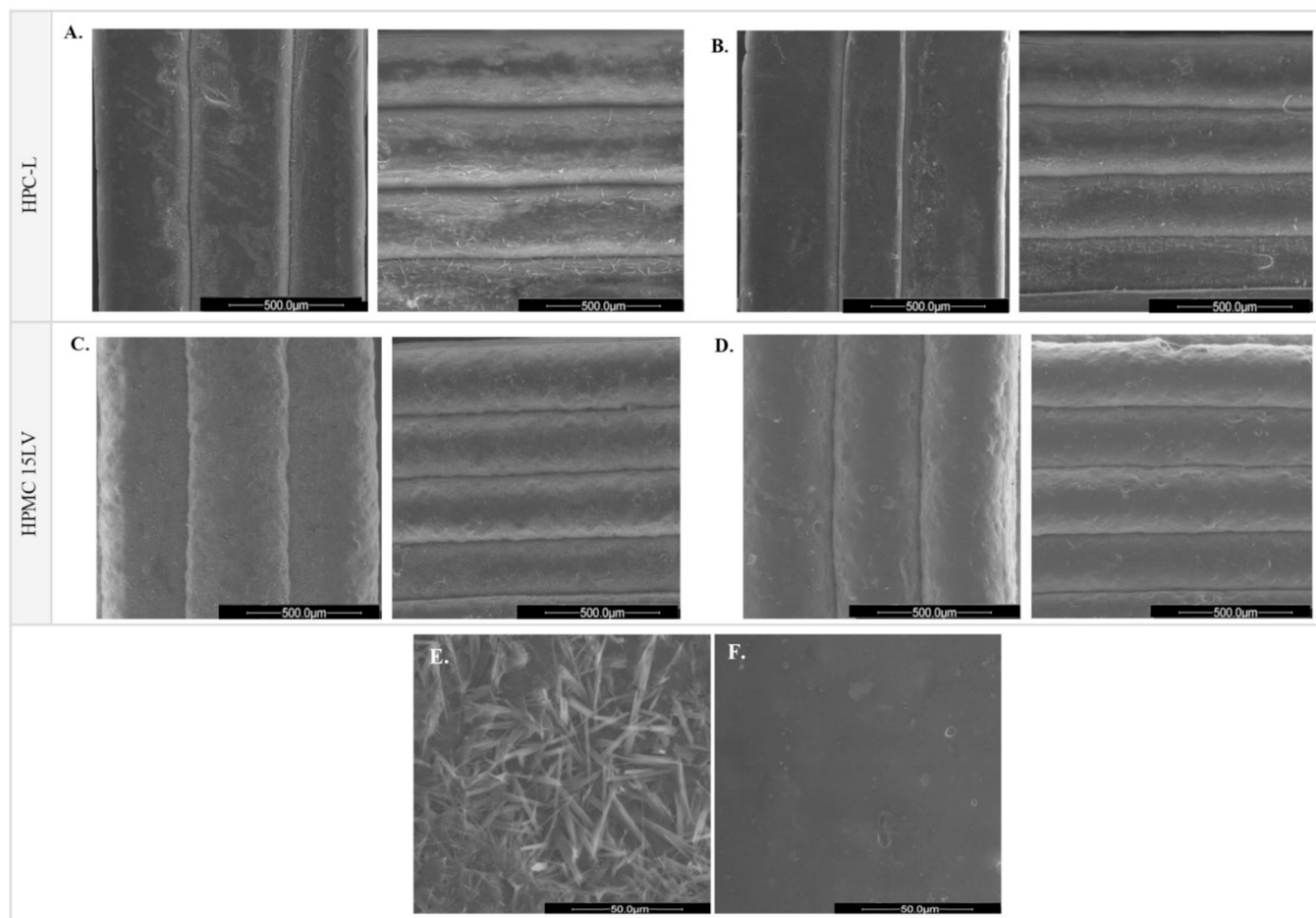


Fig. 7. In the first and second panels, SEM images of top and lateral view 3DP mini tablets showing the infill and layering. F3, F15, F9', and F19' are respectively shown in the order. In the third panel, SEM images representing caffeine-loaded (E.) vs naproxen-loaded (F.) matrices of the 3DP mini tablets showing the presence of crystalline structures.

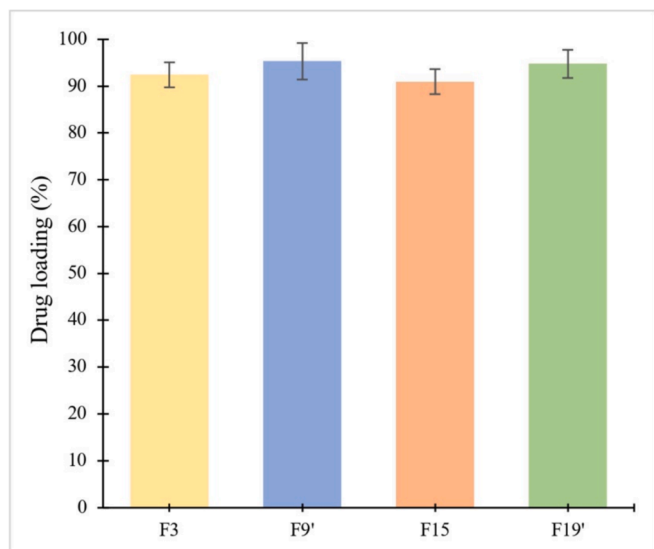


Fig. 8. Drug loading efficiency of caffeine (F3, F9') and naproxen (F15, F19') loaded mini tablets in the two different polymer matrices.

3.6. Morphological characterization by scanning electron microscopy (SEM)

SEM images shown in Fig. 7 (first and second panel) reveal a smooth surface for the 3D printed mini tablets. The layered structure appears accurate both from a top (left) and lateral view (right), confirming the accuracy of the printing process; indeed, neither overlapping nor empty spaces are observed. Moreover, in accordance with the results obtained at the XRD analysis, in Fig. 7-E, is highlighted the presence of crystalline structures in the matrix of the caffeine-loaded 3DP mini tablets, while only a slight percentage was visible in the matrix of the naproxen-loaded ones.

3.7. Uniformity of dosage units

Uniformity of mass was assessed for the mini tablets. The ones obtained from HPC-L-based formulations (F3 and F15) showed an average mass of 23.1 ± 1.8 mg and 21.2 ± 1.1 mg, respectively. While, for those obtained from HPMC 15LV (F9' and F19') the average mass was of 27.1 ± 1.6 mg and 24.3 ± 1.7 mg, respectively. European Pharmacopoeia states that individual masses of no more than two tablets can differ from the average mass by more than 10 % when it comes to uncoated single-dosage units with an average mass lower than 80 mg. Since only one tablet exceeded the 10 % limit, for both the HPC-L and HPMC 15LV-based formulations, the Eur. Ph. requirement was satisfied. Indeed, each batch's relative deviation from the mean mass was low, confirming a good reproducibility of the manufacturing method and a satisfying

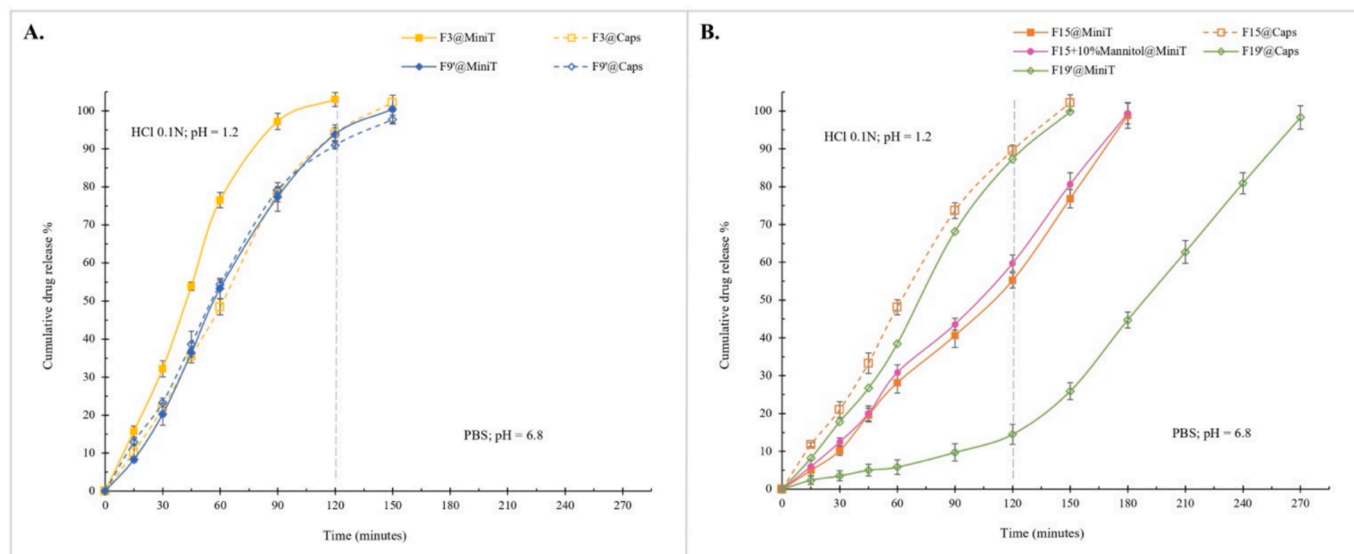


Fig. 9. Drug release profiles of size 9 capsules vs 3DP mini tablets using HPC-L and HPMC15LV matrix excipients: A) caffeine loaded and B) naproxen-loaded formulations.

Table 3

Mechanical characteristics of the 3DP mini tablets.

Formulation	Peak Force (N)	UCS (MPa)	YP (MPa)	YM (MPa)
F3	238.49 ± 8.10	18.99 ± 4.33	4.42 ± 1.01	0.24 ± 0.12
F9'	253.84 ± 13.91	21.03 ± 3.16	3.30 ± 2.03	0.21 ± 0.13
F15	210.21 ± 9.07	16.74 ± 2.68	2.06 ± 1.74	0.14 ± 0.10
F19'	217.93 ± 6.55	17.35 ± 1.72	4.03 ± 1.98	0.21 ± 0.08

control over the dosage-units' uniformity.

3.8. Drug content

The effective drug content in the 3DP mini tablets was evaluated through quantitative characterization (UV-HPLC and UV-Vis) and

referred to the theoretical API amount loaded in the powder pre-processing at the 3D printer. Drug loading efficiency was 92.41 % and 90.92 % for HPC-L based formulations (F3 and F15, respectively), and 95.32 % and 94.78 % for HPMC 15LV-based formulations (F9' and F19', respectively) as shown in Fig. 8. Overall, the amount of caffeine and naproxen loaded in the final 3DP tablets is satisfying and considered acceptable even though a small loss of drugs is present due to the manufacturing method with very limited amount of material to work with.

3.9. In vitro drug release

The release profile of the two model drugs from the different cellulose-based matrices were evaluated through dissolution studies, in accordance with the Eur. Ph. XI. As shown in Fig. 9-A (yellow plot), the

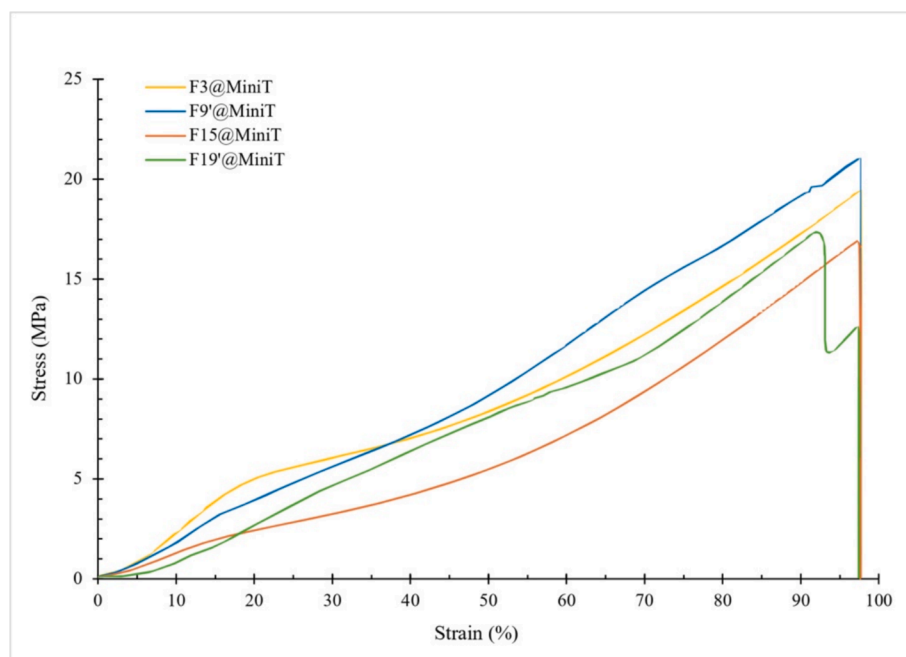


Fig. 10. Stress/strain plots of the 3DP mini tablets derived from the compression analysis.

release ratio of caffeine from the HPC-L matrix is fast and immediate, with a $77.83 \pm 2.67\%$ released in 60 min while, that of naproxen (Fig. 9, B, orange plot), is much slower, $24.86 \pm 1.70\%$ after 60 min. The variations in the release profile between caffeine and naproxen might be due to the different solubilities which are of 5 mg/mL and 1 mg/mL in water media, respectively, and to the higher physical miscibility of naproxen within the polymer in respect to caffeine, as described above in the DSC section. Moreover, the different outcome is not to be look at the presence of mannitol in the formulation as it works only as a plasticizing agent for the manufacturing process without affecting the release profile of the drug from the matrix, as shown in Fig. 9-B (pink plot), where 10 % of mannitol was added to formulation F15 and further 3D printed.

When switching to HPMC 15LV as the main polymer matrix, a slowing in the release ratio was observed, $54.41 \pm 2.70\%$ after 60 min (Fig. 9-A, blue plot) and $5.39 \pm 1.39\%$ after 60 min (Fig. 9-B, green plot) as expected.

The dissolution tests were also carried out on capsules size 9 filled with the physical blends and the resulting data compared with the ones obtained for the 3DP mini tablets as shown in Fig. 9, dotted plots. Comparing the two manufacturing methods (3DP mini tablets and conventional size 9 capsules), no significant variation was observed within the release kinetics of the oral dosage forms. Thus, suggesting that 3DP, specifically DPE, can be successfully employed to alternatively manufacture “in-house” customizable batches of mini tablets with high flexibility in terms of dosage, shape, dimensions, and materials.

3.10. Mechanical properties

A compression test was performed on the 3D printed tablets to evaluate their mechanical behaviour. In Table 3, for each formulation, the peak force (N), UCS (MPa), YM (KPa), and YP (MPa) are listed. The 100 % strain was obtained without any breakage occurring in the 3D printed mini tablets, except for formulation F19', where a breaking due to delamination occurred when 90 % of strain was reached, demonstrating the high toughness and resistance of the 3DP mini tablets. Moreover, the stress/strain graphs in Fig. 10 showed an initial elastic behaviour under the compressive force until a plastic behaviour took place. For formulations, containing 10 % of mannitol (F3, F9' and F19'), a more rigid structure (Rodríguez-Pombo, 2023) was observed, along with an increase in the YM. This direct correlation is frequently observed during mechanical tests. YM measures the resistance of a material to elastic deformation under load, thus a stiff material has a high YM and changes its shape only slightly under deforming stresses (Rodríguez-Pombo, 2023). Overall, the strength needed to reach a strain of 100 % was similar for all the tested formulations. In particular, for F15 the lowest UCS was registered along with the lowest value for the YM, underlining the higher elasticity and plasticity of the 3DP tablet.

4. Conclusions

In summary, the present study highlights the feasibility of successfully producing small batches of mini tablets with required dimensions and intended for eventual *in vivo* administration in rodents. Cellulosic excipients were selected and combined with two model drugs (e.g. caffeine and naproxen) and the blends optimized for direct powder extrusion 3D printing obtaining good physical and mechanical properties. Direct Powder Extrusion overcomes the filament production restrictions associated with Fused Deposition Modelling and streamlines the manufacturing process into a single step. However, the choice of the most suitable matrix excipient and the fine-tuning of the physical blend's characteristics is crucial step to obtain the best printing outcomes as the selected drug and polymer strongly affect the flowability of the powder mixtures and thus the printer feeding mechanism and extrudability properties. When evaluating pharmaceutical development processes DPE demonstrates to be a smart strategy able to enhance

speed, flexibility, and accessibility. Moreover, working independently from reliable sources of capsules with limited size plays a significant role when developing small batches of a novel pharmaceutical formulation and thus testing it in terms of safety and efficacy becomes more efficient and less time consuming. These advancements support efficient pre-clinical studies, streamline clinical trials, and pave the way for effective commercialization of new therapies.

CRedit authorship contribution statement

Costanza Fratini: Writing – original draft, Investigation, Formal analysis, Data curation. **Sofia Moroni:** Formal analysis. **Davide De Angelis:** Writing – review & editing, Writing – original draft, Supervision, Formal analysis, Conceptualization. **Mattia Tiboni:** Writing – review & editing, Validation, Supervision, Data curation. **Anna Giulia Balducci:** Writing – review & editing, Supervision, Methodology, Conceptualization. **Alessandra Rossi:** Writing – review & editing. **Annalisa Aluigi:** Writing – review & editing, Methodology. **Francesco Amadei:** Writing – review & editing, Resources, Conceptualization. **Luca Casettari:** Writing – review & editing, Supervision, Resources, Project administration, Methodology, Data curation, Conceptualization.

Declaration of competing interest

The authors declare that they have no known competing financial interests or personal relationships that could have appeared to influence the work reported in this paper.

Data availability

Data will be made available on request.

References

- Alhijaj, M., Belton, P., Qi, S., 2016. An investigation into the use of polymer blends to improve the printability of and regulate drug release from pharmaceutical solid dispersions prepared via fused deposition modeling (FDM) 3D printing. *Eur. J. Pharm. Biopharm.* 108, 111–125. <https://doi.org/10.1016/j.ejpb.2016.08.016>.
- Boniatti, J., et al., 2021. Direct powder extrusion 3D printing of praziquantel to overcome neglected disease formulation challenges in paediatric populations. *Pharmaceutics* 13 (8). <https://doi.org/10.3390/pharmaceutics13081114>.
- Burger, A., Henck, J.-O., Hetz, S., Rollinger, J.M., Weissnicht, A.A., 2000. Energy/temperature diagram and compression behavior of the polymorphs of D-mannitol. *Dichi, E., Legendre, B., Sghaier, M., 2014. Physico-chemical characterisation of a new polymorph of caffeine. J. Therm. Anal. Calorim.* 115 (2), 1551–1561. <https://doi.org/10.1007/s10973-013-3429-0>.
- Fanou, M., Gold, S., Muller, S., Hirsch, S., Ogorka, J., Imanidis, G., 2020. Simplification of fused deposition modeling 3D-printing paradigm: Feasibility of 1-step direct powder printing for immediate release dosage form production. *Int. J. Pharm.* 578. <https://doi.org/10.1016/j.ijpharm.2020.119124>.
- Fanou, M., Gold, S., Hirsch, S., Ogorka, J., Imanidis, G., 2020. Development of immediate release (IR) 3D-printed oral dosage forms with focus on industrial relevance. *Eur. J. Pharm. Sci.* 155. <https://doi.org/10.1016/j.ejps.2020.105558>.
- Goyanes, A., Allahham, N., Trenfield, S.J., Stoyanov, E., Gaisford, S., Basit, A.W., 2019. Direct powder extrusion 3D printing: Fabrication of drug products using a novel single-step process. *Int. J. Pharm.* 567. <https://doi.org/10.1016/j.ijpharm.2019.118471>.
- Kissi, E.O., Nilsson, R., Nogueira, L.P., Larsson, A., Tho, I., 2021. Influence of drug load on the printability and solid-state properties of 3D-printed naproxen-based amorphous solid dispersion. *Molecules* 26 (15). <https://doi.org/10.3390/molecules26154492>.
- Konta, A.A., García-Piña, M., Serrano, D.R., 2017. Personalised 3D printed medicines: Which techniques and polymers are more successful?, *MDPI AG*. doi: 10.3390/bioengineering4040079.
- Larsen, B.S., Kissi, E., Nogueira, L.P., Genina, N., Tho, I., 2024. Impact of drug load and polymer molecular weight on the 3D microstructure of printed tablets. *Eur. J. Pharm. Sci.* 192. <https://doi.org/10.1016/j.ejps.2023.106619>.
- Li, X., Kanjwal, M.A., Lin, L., Chronakis, I.S., 2013. Electrospun polyvinyl-alcohol nanofibers as oral fast-dissolving delivery system of caffeine and riboflavin. *Colloids Surf. B Biointerfaces* 103, 182–188. <https://doi.org/10.1016/j.colsurfb.2012.10.016>.
- Liu, S., Zhao, P., Wu, S., Zhang, C., Fu, J., Chen, Z., 2019. A pellet 3D printer: device design and process parameters optimization. *Adv. Polym. Tech.* 2019, 1–8. <https://doi.org/10.1155/2019/5075327>.
- Luebbert, C., Stoyanov, E., Sadowski, G., 2021. Phase behavior of ASDs based on hydroxypropyl cellulose. *Int. J. Pharm.* X 3. <https://doi.org/10.1016/j.ijpx.2020.100070>.

- Mazel, V., Delplace, C., Busignies, V., Faivre, V., Tchoreloff, P., Yagoubi, N., 2011. Polymorphic transformation of anhydrous caffeine under compression and grinding: A re-evaluation. *Drug Dev. Ind. Pharm.* 37 (7), 832–840. <https://doi.org/10.3109/03639045.2010.545416>.
- Milliken, R.L., Quinten, T., Andersen, S.K., Lamprou, D.A., 2024. In: Application of 3D Printing in Early Phase Development of Pharmaceutical Solid Dosage Forms. Elsevier B.V. <https://doi.org/10.1016/j.ijpharm.2024.123902>
- Pandey, M., et al., 2020. 3D printing for oral drug delivery: a new tool to customize drug delivery. *Drug Deliv. Transl. Res.* 10 (4), 986–1001. <https://doi.org/10.1007/s13346-020-00737-0>.
- Patel, N.G., Serajuddin, A.T.M., 2022. Moisture sorption by polymeric excipients commonly used in amorphous solid dispersion and its effect on glass transition temperature: I. Polyvinylpyrrolidone and related copolymers. *Int. J. Pharm.* 616. <https://doi.org/10.1016/j.ijpharm.2022.121532>.
- Pflieger, T., Venkatesh, R., Dachtler, M., Cooke, K., Laufer, S., Lunter, D., 2024. Influence of design parameters on sustained drug release properties of 3D-printed theophylline tablets. *Int. J. Pharm.* 658. <https://doi.org/10.1016/j.ijpharm.2024.124207>.
- Pistone, M., et al., 2022. Direct cyclodextrin-based powder extrusion 3D printing for one-step production of the BCS class II model drug nicosamide. *Drug Deliv. Transl. Res.* 12 (8), 1895–1910. <https://doi.org/10.1007/s13346-022-01124-7>.
- Pistone, M., et al., 2023. Direct cyclodextrin based powder extrusion 3D printing of budesonide loaded mini-tablets for the treatment of eosinophilic colitis in paediatric patients. *Int. J. Pharm.* 632. <https://doi.org/10.1016/j.ijpharm.2023.122592>.
- Pöstges, F., Lenhart, J., Stoyanov, E., Lunter, D.J., Wagner, K.G., 2023. Phase homogeneity in ternary amorphous solid dispersions and its impact on solubility, dissolution and supersaturation – Influence of processing and hydroxypropyl cellulose grade. *Int. J. Pharm.* X 6. <https://doi.org/10.1016/j.ijpx.2023.100222>.
- Rodríguez-Pombo, L., et al., 2023. Simultaneous fabrication of multiple tablets within seconds using tomographic volumetric 3D printing. *Int. J. Pharm.* X 5. <https://doi.org/10.1016/j.ijpx.2023.100166>.
- Sánchez-Guirales, S.A., Jurado, N., Kara, A., Lalatsa, A., Serrano, D.R., 2021. Understanding direct powder extrusion for fabrication of 3d printed personalised medicines: A case study for nifedipine minitabets. *Pharmaceutics* 13 (10). <https://doi.org/10.3390/pharmaceutics13101583>.
- Shao, X., et al., 2020. Effect of bovine bone collagen and nano-TiO₂ on the properties of hydroxypropyl methylcellulose films. *Int. J. Biol. Macromol.* 158, 937–944. <https://doi.org/10.1016/j.ijbiomac.2020.04.107>.
- Tracy, T., Wu, L., Liu, X., Cheng, S., Li, X., 2023. 3D printing: Innovative solutions for patients and pharmaceutical industry. *Int. J. Pharm.* 631. <https://doi.org/10.1016/j.ijpharm.2022.122480>.
- Zahir, M.H., et al., 2021. Preparation of a sustainable shape-stabilized phase change material for thermal energy storage based on Mg²⁺-doped CaCO₃/PEG composites. *Nanomaterials* 11 (7). <https://doi.org/10.3390/nano11071639>.
- Zaltariov, M.-F., Filip, D., Macocinschi, D., Spiridon, I., 2020. Hydroxypropyl cellulose/polyurethane blends. The behavior after accelerated ageing. A FTIR study.
- Zema, L., Melocchi, A., Maroni, A., Gazzaniga, A., 2017. In: Three-Dimensional Printing of Medicinal Products and the Challenge of Personalized Therapy. Elsevier B.V. <https://doi.org/10.1016/j.xphs.2017.03.021>